HHS Public Access

Author manuscript

J Immunol. Author manuscript; available in PMC 2016 September 15.

Published in final edited form as:

J Immunol. 2015 September 15; 195(6): 2710–2721. doi:10.4049/jimmunol.1403017.

Co-localization of a CD1d-binding glycolipid with a radiation-attenuated sporozoite vaccine in LN-resident DCs for a robust adjuvant effect

Xiangming Li[*], **Akira Kawamura**[†], **Chasity D. Andrews**[*], **Jessica L. Miller**[‡], **Douglass Wu**[§], **Tiffany Tsao**[*], **Min Zhang**, **Deena Oren**[‖], **Neal N. Padte**[*], **Steven A. Porcelli**[#], **Chi-Huey Wong**[§,**], **Stefan H. I. Kappe**[‡], **David D. Ho**[*], and **Moriya Tsuji**[*]

[*]Aaron Diamond AIDS Research Center, Affiliate of The Rockefeller University, New York, New York, 10016, USA

[†]Department of Chemistry, Hunter College of The City University of New York, New York, New York, 10065, USA

[‡]Seattle Biomedical Research Institute, Seattle, Washington, 98109, USA

[§]Department of Chemistry, The Scripps Research Institute, La Jolla, California, 92037, USA

[¶]Department of Pathology, New York University, New York, New York, USA

[‖]The Rockefeller University, New York, New York, 10065, USA

[#]Department of Microbiology and Immunology, Albert Einstein College of Medicine, Bronx, New York, 10461, USA

[**]Academia Sinica, Taipei, 115-74, Taiwan

Abstract

A CD1d-binding glycolipid, α-Galactosylceramide (αGalCer), activates invariant natural killer T (*i*NKT) cells and acts as an adjuvant. We previously identified a fluorinated phenyl ring-modified αGalCer analog, 7DW8-5, displaying nearly 100-fold stronger CD1d binding affinity. In the present study, 7DW8-5 was found to exert a more potent adjuvant effect than αGalCer for a vaccine based on radiation-attenuated sporozoites (RAS) of a rodent malaria parasite, *Plasmodium yoelii*, also referred to as irradiated *P. yoelii* sporozoites (IrPySpz). 7DW8-5 had a superb adjuvant effect only when the glycolipid and IrPySpz were conjointly administered intramuscularly (i.m.). Therefore, we evaluated the impact of distinctly different biodistribution patterns of αGalCer and 7DW8-5 on their respective adjuvant activities. While both glycolipids induce a similar cytokine response in sera of mice injected intravenously, after i.m. injection, αGalCer induces a systemic cytokine response, whereas 7DW8-5 is locally trapped by CD1d expressed by dendritic cells (DCs) in draining lymph nodes (dLNs). Moreover, the i.m. co-administration of 7DW8-5 with IrPySpz results in the recruitment of DCs to dLNs and the activation and maturation of DCs.

Address correspondence and reprint request to Dr. Moriya Tsuji, Aaron Diamond AIDS Research Center, 455 First Ave, New York, NY 10016, USA. mtsuji@adarc.org.

Disclosures

The authors have no financial conflicts of interest.

These events cause the potent adjuvant effect of 7DW8-5, resulting in the enhancement of the CD8+ T-cell response induced by IrPySpz, and, ultimately, improved protection against malaria. Our study is the first to show that the co-localization of a CD1d-binding *i*NKT-cell stimulatory glycolipid and a vaccine, like RAS, in dLN-resident DCs upon i.m. conjoin administration governs the potency of the adjuvant effect of the glycolipid.

INTRODUCTION

The eradication or acceptable control of global pathogens, including malaria, hinges upon the development of effective vaccines. One of the key strategies in realizing successful vaccines is identifying and developing new mechanism-based adjuvants. α-Galactosylceramide (αGalCer), is an extensively studied glycolipid that displays significant biological activity, including an observable adjuvant effect, that results from its binding to CD1d molecules leading to stimulation of invariant natural killer T (*i*NKT) cells (1, 2). After presentation by CD1d molecules, αGalCer activates *i*NKT cells to rapidly produce large quantities of Th1 and Th2 cytokines and subsequently induces the activation of a cascade of various immuno-competent cells, including dendritic cells (DCs), NK cells, B cells, and CD4+ and CD8+ T cells (1–4). αGalCer can therefore be utilized not only as a potential therapy for cancer, autoimmune and infectious diseases, but also as an adjuvant to enhance the efficacy of various vaccine platforms, such as adenovirus, DNA, live-attenuated pathogen, recombinant protein (5–9), and most notably, radiation-attenuated sporozoites (RAS) (10).

Several structure-activity relationship (SAR) studies of glycolipid binding to CD1d have shown that alterations to the glycolipid structure results in different biological activities (11, 12). Recently, we identified a novel αGalCer analog, 7DW8-5, which has a shorter fatty acyl chain containing an aromatic group and terminal fluorine. Compared to αGalCer, 7DW8-5 exhibited not only a more potent stimulatory activity towards *i*NKT cells and DCs, but also a higher binding affinity to both mouse and human CD1d molecules (13). We demonstrated that 7DW8-5 enhances protective anti-malaria immunity, particularly of CD8+ T cells, following intramuscular (i.m.) co-administration with an adenovirus-based malaria vaccine, and the adjuvant effect of 7DW8-5 is clearly superior when compared to its parental glycolipid, αGalCer (13). In rhesus macaques, 7DW8-5 was safe and well-tolerated as an adjuvant for an adenovirus malaria vaccine and enhanced malaria-specific CD8+ T-cell responses up to 9-fold without an adverse systemic effects (14). Recently, two independent groups have shown using a salmonella-based cancer vaccine and a recombinant *Mycobacterium bovis* bacillus Calmette-Guerin vaccines (rBCG)-based HIV vaccine models that 7DW8-5 significantly enhanced anti-tumor efficacy and SIV-specific CD8+ T cell immunogenicity, respectively (15, 16). Therefore, the glycolipid adjuvant 7DW8-5 was chosen as a lead candidate for advancing into human clinical studies with malaria and HIV vaccines (16, 17).

A malaria vaccine, based on RAS, can induce complete protection against malaria infection not only in experimental animals, but also in man (18–21), demonstrating the feasibility of effective vaccination against this disease. In mice and non-human primates, only i.v.

injection of a RAS vaccine was effective in inducing a high frequency of malaria-specific CD8+ T cells in the liver, and conferring protection in mice (22). Recent clinical trials have shown that intravenous (i.v.) immunization, but not intradermal or subcutaneous vaccination, of a RAS vaccine induced sterile protection against malaria (22, 23), and a majority of protected subjects were found to have a higher number of CD8+ T cells producing IFN-γ in their blood. In view of the fact that there are currently a number of RAS vaccines (22, 23) in Phase I/II trials, we believe it is of utmost importance to identify an adjuvant that can enhance the efficacy of current candidate a RAS-based malaria vaccine. In fact, we have previously shown that co-administration of αGalCer with irradiated *Plasmodium yoelii* sporozoites (IrPySpz), a *Plasmodium yoelii* RAS vaccine, caused an enhancement in the protective anti-malaria immunity induced by IrPySpz, which was abolished in mice lacking CD1d molecules or Vα14 *i*NKT cells (10).

In this present study, we first determined a superior adjuvant effect of 7DW8-5 over αGalCer on the T-cell immunogenicity and protective efficacy of IrPySpz, upon conjoint administration of the glycolipid and IrPySpz by i.m. We then studied i.m. injection of 7DW8-5 and IrPySpz resulting in co-localization in draining lymph node (dLN)-resident DCs and their subsequent activation and maturation. Then, we further investigated whether the unique biodistribution of 7DW8-5 co-localizing with IrPySpz vaccine would ultimately result in the enhancement of the T–cell immunogenicity and protective efficacy of the malaria vaccine *in vivo*. Understanding the mechanism of action of 7DW8-5 will have important implications for the clinical application of 7DW8-5 as an adjuvant.

MATERIALS AND METHODS

Parasites

A parasite line of transgenic *P. yoelii* sporozoites expressing GFP-luciferase fusion protein, PySpz(GFP-Luc) was generated as described (24). Wild type *P. yoelii* sporozoites (PySpz) 17 XNL strain and PySpz(GFP-Luc) were maintained in the insectary facility of the Division of Parasitology, Department of Microbiology at New York University School of Medicine. Sporozoites were obtained from dissected salivary glands of infected *Anopheles stephensi* mosquitoes 2 weeks after infective blood meal. For immunization, PySpz were radiation-attenuated by exposing them to 12,000 rad.

Mice

Six to 8-week old female BALB/c mice were purchased from Taconic (Germantown, NY). C.129S2-*Cd1*^{tm1Gru}/J mice (25), a homozygous strain that lacks both CD1d1 and CD1d2 genes, and C.FVB-Tg(Itgax-DTR/EGFP)57Lan/J mice (26), a CD11c-DTR transgenic mice expressing a simian Diphtheria Toxin Receptor (DTR)-Enhanced Green Fluorescent Protein (EGFP) fusion protein under the control of the *Itgax* (or CD11c) promoter, were purchased from the Jackson Laboratory (Bar Harbor, ME). After i.p. injection of 100 ng Diphtheria Toxin (MP Biomedicals, Aurora, OH) to CD11c-DTR mice, CD11c^{+} DCs were ablated for at least 24 hr while preserving other immune-competent cells, as we previously published (27). All of mice were maintained under standard conditions in The Laboratory Animal Research Center of The Rockefeller University, and the protocol was approved by the

Institutional Animal Care and Use Committee (IACUC) at The Rockefeller University (Assurance # A3081-01).

Assessment of antigen-specific CD8+ T-cell responses

The numbers of antigen-specific, IFN-γ-secreting CD8+ T cells in the spleens of immunized mice were determined by an ELISpot assay, using a synthetic 9-mer peptide, SYVPSAEQI, corresponding to the CD8+ T cell epitope within the respective antigen, as previously described (10, 13). The peptide was synthesized by Biosynthesis, Inc. (Lewisville, TX, USA).

Sporozoite challenge and assessment of protection

P. yoelii (17XNL strain) sporozoites were obtained from dissected salivary glands of infected *Anopheles stephansi* mosquitoes 2 weeks after infective blood meal. Sporozoite challenge experiments were performed as described previously (10, 13). Briefly, immunized mice, as well as non-immunized mice as a control, were administered i.v. with 100 live *P. yoelii* sporozoites, and parasitemia were monitored from day 3 to 10 post challenge, by detecting the presence of parasites in thin blood smears to assess complete protection against malaria. In some experiments, when a modest level of inhibition of liver stage development (<90%) was anticipated, immunized and non-immunized mice were injected with 2×10^4 live *P. yoelii* sporozoites via tail vein, and 42 hr later, the parasite burden in the liver was determined by measuring parasite-specific ribosomal RNA using 7300 Real-Time PCR System (Applied Biosystems, Foster City, CA, USA). Parasite burden was described as a ratio of the absolute copy number of parasite ribosomal RNA to that of mouse GAPDH mRNA (10, 13, 24, 28–31).

Amounts of a glycolipid in the sera upon its i.v. or i.m. injection

The concentration of glycolipid in sera was measured by a modified method described previously (32). Mice (n=24/group) were administered 1 μg αGalCer or 7DW8-5 by i.m. or i.v. injection. After 2, 6, 12 and 24 hr, six mice from each group were sacrificed, and sera were collected. Serial dilutions of individual sera were incubated with 3×10^4 murine 1.2 *i*NKT hybridoma cells and 3×10^4 A20 cells expressing mouse CD1d (A20-mCD1d) in a 96-well plate at 37°C. To generate a standard curve, αGalCer and 7DW8-5 were serially diluted in naïve serum and co-cultured with *i*NKT hybridoma and A20-mCD1d cells. Naïve sera were used as negative controls. After 16 hr, supernatants were collected and IL-2 concentrations were determined using the mouse IL-2 ELISA kit (BioLegend, San Diego, CA). αGalCer and 7DW8-5 serum concentrations were calculated from standard curves generated from the serially diluted glycolipids.

Glycolipid labeling

Amine-modified αGalCer and 7DW8-5 were synthesized by Aptuit LLC (Greenwich, CT). Five-hundred μg of glycolipid and 500 μg of the succinimide ester of either Alexa Fluor 680 (AF680)(Molecular Probes, Carlsbad, CA) or BODIPY Texas Red-X (BTR)(Molecular Probes) were dissolved in anhydrous pyridine (100 μl). The reaction proceeded at room temperature in the dark for 24 hr before the pyridine was removed *in vacuo*. The product

was then purified by silica gel chromatography and quantified by the UV absorption of the attached dye. The product formation was confirmed by mass spectrometry as shown below. AF680-αGalCer (Rf 0.43; methanol-dichloromethane 3:7 (v/v), HRESIMS (m/z): cald for C93H124BrFN3O21S2 [M-2H]-2 891.8681, found 891.8686); AF680-7DW8-5 (Rf 0.34; methanol-dichloromethane 3:7 (v/v), HRESIMS (m/z): cald for C102H151BrN3O21S2 [M-2H]-2 949.9752, found 949.9756); BTR-αGalCer (Rf 0.57; methanol-dichloromethane 1:9 (v/v), HRESIMS (m/z): cald for C86H141BF2N5O16S [M+H]+ 1581.0150, found 1581.0162); BTR-7DW8-5 (Rf 0.46; methanol/dichloromethane = 1:9, HRESIMS (m/z): cald for C77H114BF3N5O16S [M+H]+ 1464.8021, found 1464.8029).

IVIS imaging

Mice (n=5/group) were injected into anterior tibialis muscles of both legs with 5 μg AF680-αGalCer, AF680-7DW8-5 or AF680. Mice also received i.m. administration of IrPySpz(GFP-Luc) by i.m. or i.v. At the indicated time points, mice were anesthetized with isoflurane (Baxter, Deerfield, IL) and imaged with IVIS Lumina imaging system (Caliper, Hopkinton, MA) using cy5.5 filter. Tissue-specific autofluorescence and background were subtracted with Image Math software (Caliper). Fluorescence intensities in the region of interest (ROI) were quantified with ROI measurement tools (Caliper).

Immunohistofluorescence of LNs

BALB/c or CD1d$^{-/-}$ mice (n=5/group) were treated with 2 μg BTR-αGalCer or BTR-7DW8-5 by i.m. injection. After 8 hr, popliteal lymph nodes (PLNs) were harvested, fixed with 2% paraformaldehyde for 30 min, washed three times, and permeabilized with Perm/Fix buffer (BD Bioscience, San Jose, CA) for 15 min. The tissues were washed with Perm/Wash buffer and blocked with 5% goat sera and 2% BSA for 30 min. After washing, the tissues were stained either with antibody against B220, F4/80, or CD11c (BioLegend) at 4°C overnight. Primary antibodies were detected with AF647 labeled goat anti-mouse secondary antibody (Invitrogen, Carlsbad, CA) for 1 hr. After washing, the tissues were imaged with LSM510 confocal microscope (Zeiss, Oberkochen, Germany).

Detection of glycolipid:mCD1d complex by L363 antibody

Two μg of rat anti-mouse IgG1 antibody was incubated with anti-rat IgG κ chain antibody coated microbeads (BD Bioscience) for 2 hr. After washing, microbeads were incubated with 1 μg of mCD1d:mIgG1 dimer for 2 hr, followed by washing and loading of microbeads with 2 μg of αGalCer or 7DW8-5 at 37°C overnight. Then, microbeads were washed and stained with serially diluted AF647-labeled L363 antibody for 30 min, and then samples were analyzed with BD LSRII flow cytometer. The binding kinetics of L363 antibody staining was fit using GraphPad Prism 4.0 software.

Infiltration of CD11c+MHC-II+ DCs to PLNs and their level of CD1d expression and activation/maturation status

Mice (n=4/group) were administered 1 μg αGalCer or 7DW8-5 by i.m. injection, and a single cell suspension was prepared from PLNs at 16 hr p.i. The percentage of CD11c +MHC-II+ DCs among total LN cells was determined by positive staining with both anti-

CD11c and anti-MHC-II antibodies. The activation/maturation status of PLN-resident DCs was determined by the expression level of MHC-II and CD86. The expression level of CD1d was also determined. Cells were stained with PE-labeled anti-mouse CD11c antibody, Pacific Blue-labeled anti-mouse MHC-II antibody, AF647-labeled anti-mouse CD86 antibody, and PerCP-Cy5.5-labeled anti-mouse CD1d antibody (all from BioLegend) at 4°C for 1 hr. Cells were washed and analyzed using a BD LSRII flow cytometer with FACSDiva software.

Data Analysis

For most of the studies, statistical analysis of experimental and control data were evaluated by one-way ANOVA and Student *t*-test. For protection studies, *P* value was calculated by $\chi 2$ test, using 2 × 2 contingency table (degree of freedom = 1). $p \leq 0.05$ was considered significant.

RESULTS

The potency of the adjuvant effect of 7DW8-5 depends on the route of its administration

Our previous studies have shown the high affinity for CD1d and stimulatory activity for *i*NKT cells, of an αGalCer analog, 7DW8-5, which ultimately yield potent adjuvant activity against viral and DNA vaccines (13). A *P. falciparum* RAS vaccine stimulated protective anti-malarial immunity in several clinical trials (22, 23) leading us to determine the adjuvant effects of 7DW8-5 and αGalCer, with a *P. yoelii* RAS vaccine, IrPySpz in mice.

We first immunized mice with IrPySpz alone or together with either glycolipid by intramuscular (i.m.) or intravenous (i.v.) administration. Twelve days or 6 weeks later, we isolated splenocytes from immunized mice and determined the level of CD8+ T-cell response specific for a major malaria antigen, *P. yoelii* circumsporozoite antigen (PyCS) by counting the relative number of PyCS-specific CD8+ T cells with an IFN-γ ELISpot assay (Fig. 1A). I.m. co-administration of 7DW8-5 greatly enhanced PyCS-specific CD8+ T-cell response induced by IrPySpz vaccine. The 7DW8-5 co-administration's enhancement was more evident than αGalCer co-administration not only 12 days after but also 6 weeks after immunization. The superior adjuvant effect of 7DW8-5 over αGalCer was diminished when either glycolipid was co-administered with IrPySpz i.v. (Fig. 1A). It is noteworthy that the i.m. immunization regimen appears less effective in eliciting PyCS-specific CD8+ T-cell response than IrPySpz immunization by i.v. conjointly with either αGalCer or 7DW8-5 (both day 12 and week 6 post immunization). In parallel, we determined the percentage of $CD8\alpha^{low}CD11a^{high}$ CD8+ T cells by flow cytometric analysis (Fig. 1B), in view of a study showing the association of a surrogate activation marker - $CD8\alpha^{low}CD11a^{high}$ - of CD8+ T cells induced by IrSpz with protection (33). We observed a similar trend with this method, specifically a superior adjuvant effect of 7DW8-5 compared to αGalCer when the glycolipids were co-injected with IrPySpz by i.m. but not by i.v. (Fig. 1B). When we determined the level of protection by the presence or absence of parasitemia in thin blood smears, we found that 3 out of 5 mice received 7DW8-5 co-administration i.m. with IrPySpz were protected against malaria challenge 12 days after immunization (Table I). The best

protection was observed when mice were administered i.v. with IrPySpz conjointly with αGalCer (4 out of 5 mice were protected: Table I).

Next, we investigated whether conjoint (same limb) i.m. administration is crucial for the glycolipids to display their adjuvant effects. For this purpose, IrPySpz was administered i.m.; i) conjointly with either glycolipid i.m.; ii) with either glycolipid by i.v. (tail vein) route; or iii) with either glycolipid i.m. on the opposite limb. Then, we determined the level of PyCS-specific CD8+ T cell response by an IFN-γ ELISpot assay (Fig. 1C), as well as the level of anti-malaria protection (Table II). Similarly to earlier experiments that we observed (Fig. 1A), 7DW8-5 exerted an adjuvant effect significantly stronger than αGalCer, when either glycolipid was conjointly administered i.m. with IrPySpz (Fig. 1C). Furthermore, upon malaria challenge, i.m. co-administration of 7DW8-5 enhanced the protective anti-malaria immunity induced by IrPySpz more than αGalCer, and the degree of protection was same as that induced by i.v. administered IrPySpz (9 out of 10 mice protected; Table II). However, when IrPySpz was administered by i.m. route and each glycolipid was administered by i.v. route, both glycolipids only modestly enhanced the PyCS-specific CD8+ T-cell response (Fig. 1C) and marginally enhanced the protective efficacy of IrPySpz vaccine (Table II). Interestingly, when IrPySpz and glycolipids were administered i.m. on opposite limbs, the adjuvant effect of 7DW8-5 was completely abolished, while αGalCer moderately enhanced the malaria-specific CD8+ T-cell response and protective efficacy of the IrPySpz vaccine (Fig. 1C, Table II). When we determined the level of PyCS-specific CD8+ T-cell response by an IL-2 ELISpot assay (Fig. 1D), we again observed a superior adjuvant effect of 7DW8-5 over αGalCer only when IrPySpz and glycolipid were conjointly administered by i.m. The number of IL-2-secreting CD8+ T cells in response to PyCS is similar or slightly higher than that of IFN-γ-secreting CD8+ T cells, suggesting that a majority of PyCS-specific CD8+ T cells secrete both cytokines. Collectively, these results highlight the importance of conjoint administration of a RAS vaccine and 7DW8-5 for maximizing vaccine efficacy.

7DW8-5 does not spread in circulation or cause systemic cytokine production following intramuscular injection

We determined IFN-γ serum concentrations following i.v. or i.m. injection of 7DW8-5 or, αGalCer. A robust IFN-γ response was observed that peaked 12 hr post injection (p.i.) in mice injected i.v. with either glycolipid (Fig. 2A). However, following i.m. administration, IFN-γ was only detected in the sera of mice injected with αGalCer, but not with 7DW8-5 (Fig. 2B). When we determined glycolipid serum concentrations following its i.v. injection, comparable serum glycolipid concentrations were observed after i.v. injection peaking at 2 hr p.i. and returning to basal levels at 24 hr p.i. (Fig. 2C). However, i.m. injection of the glycolipids resulted in lower αGalCer serum concentrations than were observed following i.v. administration, and, markedly, no 7DW8-5 was detected in the sera (Fig. 2D). Thus, following i.m. injection, αGalCer spreads into the blood generating a potent systemic IFN-γ response, while 7DW8-5 fails to reach systemic circulation, leading to an undetectable systemic IFN-γ response. These results indicated that the moderate adjuvant effects of 7DW8-5 and αGalCer following i.v. injection and αGalCer following i.m. injection may be due to the induction of systemic immune responses. However, i.m. injection of 7DW8-5

induced a localized, not systemic, immune response probably resulting in its superior adjuvant effect.

7DW8-5, but not αGalCer, is retained locally following i.m. injection

Based on the absence of 7DW8-5 in the sera following i.m. injection and considering that 7DW8-5 has a much stronger binding affinity to human CD1d (hCD1d) and mouse CD1d (mCD1d) than αGalCer (13), it is plausible that following i.m. injection, 7DW8-5 is efficiently captured by CD1d-expressing antigen-presenting cells (APCs) near the injection site and retained in the draining lymph nodes (dLNs). In contrast, the weaker binding affinity of αGalCer for CD1d renders it more likely to spread into systemic circulation, leading to our hypothesis that 7DW8-5 and αGalCer display distinct biodistribution patterns upon i.m. injection.

To test this hypothesis, infrared fluorochrome Alexa Fluor 680 (AF680)-labeled glycolipids were synthesized by introducing modifications at the 6′-OH of the galactose head group (Supplemental Fig. 1A), a modification site which we previously demonstrated has no significant effect on the binding of the glycolipids to CD1d or the TCR of *i*NKT cells (34). The binding affinity and biological activity of the labeled glycolipids, AF680-αGalCer and AF680-7DW8-5, was similar to the unmodified glycolipids (Supplemental Fig. 1B–E). Labeled glycolipids were injected i.m. into the anterior tibialis muscles of both legs of BALB/c mice, and biodistribution was determined using a whole body *in vivo* imaging system (IVIS). Following AF680-7DW8-5 injection, fluorescence persisted for 12 hr (yellow arrows; Fig. 3A) but decreased by 24 hr, and the anatomical site of the fluorescence correlates with the popliteal lymph nodes (PLNs). Punctate, intensely localized, fluorescent regions were not observed in mice injected with either AF680-αGalCer or AF680 (Fig. 3A, 3B). The route of administration affected the biodistribution of only AF680-7DW8-5; its i.m. injection, but not i.v. injection, resulted in locally accumulated fluorescence at 8 hr p.i. (Fig. 3C, 3D). These results show that 7DW8-5 is retained locally, i.e. PLNs, after i.m. injection, while αGalCer distributes more systemically.

To evaluate the role of CD1d molecules in retaining 7DW8-5 locally, AF680-labeled glycolipids were injected i.m. into CD1d-deficient ($CD1d^{-/-}$) mice that also lack *i*NKT cells (25). Punctate fluorescence was not observed (Fig. 3E, 3F) illustrating that trapping 7DW8-5 near the site of injection is CD1d-dependent. Next, the biodistribution of glycolipids was evaluated in CD11c-DTR transgenic mice lacking DCs (26), the primary APCs for glycolipids (9, 27), and punctate fluorescence was not observed with either glycolipid (Fig. 3E, 3F). Collectively, these results indicate that the localized biodistribution of 7DW8-5 following i.m. injection is dependent on DCs expressing CD1d molecules, suggesting that CD1d-expressing DCs residing in the dLNs may trap 7DW8-5.

Efficient CD1d-dependent trapping of 7DW8-5 by PLN-resident DCs

To confirm the IVIS results, whole PLNs were harvested and imaged to detect the fluorescent-labeled glycolipid. For this experiment, glycolipids were first labeled with a fluorochrome BODIPY-Texas Red (BTR) (Supplemental Fig. 1A), as previously described (35), and their CD1d binding was similar to unlabeled glycolipds (Supplemental Fig. 1B,

1C). BALB/c mice were injected i.m. into anterior tibialis muscles with BTR-labeled glycolipids, and 8 hr later the PLNs were harvested and visualized by confocal microscopy. BTR-7DW8-5, but not BTR-αGalCer, was retained in the PLNs (Fig. 3G). However, neither BTR-labeled glycolipid was retained in the PLNs of $CD1d^{-/-}$ mice that lack *i*NKT cells (Fig. 3G), indicating that the specificity of 7DW8-5 for CD1d was necessary for its restricted localization.

We examined the contribution of B cells, macrophages, and DCs, all of which express CD1d, in presenting 7DW8-5. PLNs were harvested as described above, stained with the appropriate cell makers and visualized by confocal microscopy. Co-localization was only observed in the PLNs of BTR-7DW8-5-treated mice stained with the CD11c DC marker (Fig. 3H), not when stained with B cell or macrophage markers. As expected by the IVIS experiment (Fig. 3A–F), αGalCer was not retained locally. Therefore, no BTR-αGalCer signal was observed in the PLNs (Fig. 3G, 3H). These results indicate that DCs are the primary cell responsible for trapping/presenting 7DW8-5 in dLNs upon i.m. injection.

PLN-resident DCs present 7DW8-5 and induce *i*NKT activation following i.m. injection

We examined the impact of the glycolipids biodistribution on their presentation by APCs *in vivo*. For these studies, L363, an antibody that recognizes each glycolipid/mCD1d complex with comparable affinity (Supplemental Fig. 2A, 2B), was used to quantify the glycolipid bound to mCD1d (36). After either glycolipid was administered i.m. or i.v. to mice, PLNs and spleens were harvested. Macrophages, B cells and DCs were identified by gating for $CD11c^{-}CD11b^{+}F4/80^{+}$, $B220^{+}CD11c^{-}F4/80^{-}$, and $CD11c^{+}MHC\text{-}II^{+}F4/80^{-}$, respectively (Supplemental Fig. 2C), and the mean fluorescence intensity (MFI) of L363 was measured by flow cytometry. Following i.m. administration of 7DW8-5, only DCs in PLNs but not in spleen, displayed a strong binding of 7DW8-5 by CD1d as indicated by a nearly 5-fold increase in L363 MFI (Fig. 4A, Supplemental Fig. 2D). In contrast, following i.m. injection of αGalCer, L363 staining of splenic DCs was greater than that of PLN-resident DCs (Fig. 4A, Supplemental Fig. 2D). However, following i.v. administration, both glycolipids induced similar levels of L363 binding on splenic DCs without inducing detectable binding on PLN-resident DCs (Fig. 4B, Supplemental Fig. 2E). Macrophages and B cells from both tissues were not positive for L363 staining following injection of either glycolipid regardless of the administration route (Fig. 4A, 4B, Supplemental Fig. 2D, 2E). Taken together, following i.m. injection, 7DW8-5 is primarily presented by CD1d on dLN-resident DCs, while αGalCer primarily spreads into systemic circulation, as evidenced by its binding to CD1d on splenic DCs.

Next, we investigated the effect of the different glycolipid biodistribution patterns on the activation of *i*NKT cells *in vivo*. PLNs and spleens were harvested from mice after i.m. or i.v. injection of each glycolipid. Cells were isolated and stained with αGalCer-loaded mCD1d dimer and anti-CD3 antibody to gate *i*NKT cells (Supplemental Fig. 3A), followed by staining with anti-CD69 antibody to determine the activation status. Upon i.m. injection of αGalCer, *i*NKT cells in the spleen displayed a higher level of activation compared to those in PLNs (Fig. 4C). In contrast, i.m. administration of 7DW8-5 resulted in *i*NKT cell activation in PLNs but not in spleen (Fig. 4C, Supplemental Fig. 3B). Upon i.v.

administration, both glycolipids induced a high level splenic *i*NKT cell activation, but failed to activate PLN-resident *i*NKT cells (Fig. 4D, Supplemental Fig. 3C). Neither glycolipid induced early *i*NKT cell activation in spleens or PLNs of CD11c-DTR transgenic mice lacking DCs (Supplemental Fig. 3B, 3C). These results collectively indicate that i.m. administered 7DW8-5 was trapped and presented by CD1d expressed by LN-resident DCs, leading to rapid activation of *i*NKT cells in LNs. However, i.m. delivered αGalCer spread systemically and was presented by CD1d expressed by splenic DCs inducing the activation of splenic *i*NKT cells.

Kinetics and molecular modeling of 7DW8-5 and CD1d binding

Compared with αGalCer, 7DW8-5 binds CD1d with nearly 30–80-fold stronger affinity than αGalCer (13), and this may impact the localized biodistribution of 7DW8-5 at a molecular level. The kinetics of glycolipid binding to CD1d was determined by incubating A20-mCD1d cells with an excess of each glycolipid and staining with L363 antibody at the indicated time points. The time required for 50% of mCD1d to be bound by 7DW8-5 ($T_{1/2}$ = 23.7 ± 3.9 min) was nearly one tenth of that by αGalCer ($T_{1/2}$ = 377 ± 22 min) (Supplemental Fig. 4A), indicating that 7DW8-5 binds mCD1d much faster than αGalCer. To better understand the binding affinities, modeling of the 7DW8-5/mCD1d complex was performed based on the crystal structures of αGalCer analogs/mCD1d complex (Supplemental Fig. 4B). Superimposed structures illustrated that the phenyl ring of the 7DW8-5 acyl chain fits in the mCD1d binding pocket in a more stretched, rigid orientation possibly increasing the surface interaction between the lipid chain and the hydrophobic A′ pocket. The bulk of the phenyl ring restrains the acyl chain in the pocket compared with the single lipid chain of αGalCer, which is flexible allowing easier exit from the binding pocket. Furthermore, 7DW8-5 potentially forms stacking interactions with Phe70 of mCD1d in the A′ pocket (Supplemental Fig. 4B), which may increase stability and binding affinity. The fluoride group also has the potential to interact with residues of the binding pocket wall. Taken together, 7DW8-5 binds CD1d more rapidly than αGalCer, and modeling suggests that the molecular features of 7DW8-5 improve 7DW8-5/mCD1d complex stability.

Localized biodistribution of 7DW8-5 recruits DCs and increases DC activation/maturation leading to its enhanced adjuvant effect

NKT cells induce the activation/maturation of DCs upon glycolipid binding to CD1d expressed on DCs (3, 4, 9). In view of our biodistribution studies, it is likely that early activation of *i*NKT cells in PLNs induced by i.m. injected 7DW8-5 (Fig. 4C) may attract more DCs to LNs. To test this hypothesis, mice were injected i.m. with glycolipids, and the percentage of DCs among total PLN lymphocytes was determined. Six hr p.i., the percentage of DCs in PLNs significantly increased following 7DW8-5 administration, but not αGalCer.Furthermore, at 24 hr p.i., the percentage of DCs continued increasing with significantly more DCs detected in the 7DW8-5-treated mice (Fig. 5A). These data indicate that i.m. injection of 7DW8-5 recruits more DCs to the local dLNs through early *i*NKT cell activation.

Next, in view of a study showing that αGalCer increases CD1d expression on DCs *in vivo* upon i.p. injection (28), we sought to determine if the glycolipids affect the level of CD1d

expression differently. PLN-resident DCs from mice administered 7DW8-5 i.m. showed significantly higher CD1d, CD86 and MHC-II expression than αGalCer (Fig. 5B–D), thus indicating a higher level of activation/maturation by PLN-resident DCs. To determine whether the localized biodistribution of 7DW8-5 improved the antigen presentation capability of PLN-resident DCs following i.m. injection, PLN-resident DCs were isolated from mice injected with each glycolipid and loaded with a synthetic peptide, SYVPSAEQI, which corresponds to an immunodominant $CD8^+$ T-cell epitope of PyCS antigen. These peptide-loaded DCs were then adoptively transferred into naïve mice, and the PyCS-specific CD8+ T-cell response was determined by an IFN-γ ELISpot assay (Fig. 5E). As shown in Fig. 5F, DCs isolated from 7DW8-5-injected mice induced nearly a 4-fold higher PyCS-specific CD8+ T-cell response than DCs isolated from naïve mice, whereas DCs isolated from αGalCer-injected mice enhanced PyCS-specific CD8+ T-cell response by only 2-fold.

7DW8-5 exerts a potent adjuvant effect for irradiated sporozoite vaccine by co-localizing with PLN-resident antigen-presenting DCs and facilitating their activation/maturation

The potent efficacy of a RAS-based malaria vaccine in recent human trials (22, 23) led us to investigate the mechanisms by which 7DW8-5 exerts a stronger adjuvant effect than αGalCer for a RAS vaccine. The *in vivo* localization of *P. yoelii* RAS vaccine, IrPySpz, was first compared upon i.m. versus i.v. administration, using transgenic PySpz expressing a GFP-luciferase fusion protein, PySpz(GFP-Luc) (24). As shown in a number of studies (24, 37, 38), luciferase expression was strongly detected in the liver following i.v. administration (Fig. 6A). Following i.m. immunization, punctate luciferase expression was detected at a location coinciding with PLNs (Fig. 6A), indicating that IrPySpz localize in the same area as AF680-labeled 7DW8-5 (Fig. 3A, 3C, 3E). Following immunization with IrPySpz(GFP-Luc), PLN-resident lymphocytes expressing GFP were only CD11c+, but not F4/80+ or B220+ (Fig. 6B), indicating that DCs are the main cells presenting PySpz antigens. 7DW8-5 co-administered with IrPySpz(GFP-Luc) recruited 2-fold more GFP^+ DCs than αGalCer (Fig. 6C) and significantly increased the expression of CD86 and MHC-II molecules (Fig. 6D, 6E).

The most important aspect of our studies was to determine the impact of the increased number and activation state of PLN-resident PySpz+ DCs by 7DW8-5 co-administration on the protective anti-malaria immunity. Therefore, to investigate this aspect, CD11c+ PLN-resident DCs were isolated from BALB/c mice shortly after being immunized with IrPySpz alone, or together with either glycolipid, and then adoptively transferred to naïve BALB/c mice (Fig. 6F). Ten days after the adoptive transfer, an IFN-γ ELISpot assay using peripheral blood of DCs-transferred mice, showed that the highest PyCS-specific CD8+ T cells were induced in mice receiving adoptive transfer of PLN-resident DCs isolated from mice immunized with IrPySpz together with 7DW8-5, compared with those immunized with IrPySpz alone or IrPySpz plus αGalCer (Fig. 6G). To determine the level of protective anti-malaria immunity, these groups of transferred mice were challenged with PySpz. Adoptive transfer of PLN-resident DCs isolated from mice immunized with IrPySpz co-administered with 7DW8-5 induced the highest level of protective immunity against malaria compared to mice immunized with IrPySpz alone or IrPySpz with αGalCer (Fig. 6H). Taken together, these results indicate that 7DW8-5 co-administered with a RAS vaccine strongly enhances

not only the T-cell immunogenicity, but also the protective anti-malaria immunity, by improving the quantity/quality of malaria antigen-presenting PLN-resident DCs.

DISCUSSION

We previously identified a new CD1d-binding, *i*NKT cell-stimulating glycolipid, named 7DW8-5, which displays a potent adjuvant activity, enhancing malaria-specific CD8+ T-cell response, when co-administered i.m. with an adenovirus-based malaria vaccine (13). Although 7DW8-5 and its parental glycolipid, αGalCer, have similar chemical structures, differing only in the fatty acyl chain, 7DW8-5 stimulates *i*NKT cells more intensely and induces more DC activation/maturation than αGalCer *in vitro* (13). The binding affinity of 7DW8-5 to CD1d molecules is higher than that of αGalCer, and 7DW8-5 can exert a 100-fold higher dose sparing effect of glycolipid than αGalCer *in vivo* (13). Numerous studies have addressed the mechanisms by which CD1d-binding, *i*NKT cell-stimulating glycolipids, such as αGalCer, display their adjuvant effect at a molecular level (5–10), ultimately acting as a vaccine adjuvant; however, little, if anything, is currently known about how this enhances the adaptive immune responses *in vivo* at whole body level. First, we determined that 7DW8-5 displays an adjuvant effect superior to αGalCer's, enhancing the T-cell immunogenicity and protective efficacy of IrPySpz, particularly when the glycolipid and IrPySpz are conjointly administered by i.m. (Fig. 1). Then, we found sharply contrasting systemic cytokine production profiles induced by i.m. administration of two structurally related glycolipids (Fig. 2A), leading us to investigate the biodistribution of the glycolipids in more detail.

We used two different fluorophores, AF680 and BTR, which attach at the 6′-OH position of the galactose head of the glycolipids, without affecting the binding of the glycolipids to CD1d or the TCR of *i*NKT cells (Supplemental Fig. 1) (34). The different excitation and emission wavelengths of the fluorophores allowed us to comprehensively evaluate the biodistribution of the glycolipids both with whole body imaging and tissue analyses. These studies confirmed that two glycolipids exhibit distinct biodistribution patterns following i.m. administration. 7DW8-5, but not αGalCer, distributed locally within PLNs and preferentially bound CD1d molecules on DCs (Fig. 3). While the fluorophore-labeled glycolipid allows tracking of the glycolipid biodistrubtion, it does not directly prove an association of the glycolipid with a CD1d molecule on DCs. Therefore, we used an antibody, L363, which recognizes the epitope consisting of the glycolipid and mCD1d complex (36) to verify that 7DW8-5 binds CD1d molecules expressed by DCs, but not by other APCs in the dLNs (Fig. 4A). This supports the results obtained by whole body imaging and tissue analysis (Fig. 3). Conversely, αGalCer, following i.m. administration, spreads to systemic circulation and bound splenic DCs, albeit to a lesser degree than the binding observed following i.v. administration (Fig. 4A, 4B).

It is evident from these studies that 7DW8-5 binds CD1d, particularly those expressed by dLN-resident DCs, thus leading to its unique and localized biodistribution. This preferential binding by 7DW8-5 may be due to two factors: 1) the higher binding affinity of 7DW8-5 to CD1d molecules and 2) the induction of increased CD1d expression by 7DW8-5. Concerning the first factor, in addition to the higher binding affinity of 7DW8-5 to CD1d

molecules than αGalCer (13), we determined that the on-rate of 7DW8-5 binding to mCD1d molecules is more than 10 times greater than αGalCer's (Supplemental Fig. 4A). To determine why 7DW8-5 binds CD1d with more affinity and faster than αGalCer, we modeled the 7DW8-5/mCD1d complex interaction based on the crystal structures of αGalCer analogs/mCD1d complexes previously published (39, 40). 7DW8-5 appears to bind more tightly than αGalCer to the binding pockets, particularly the A′-pocket, of mCD1d molecule, thus improving the 7DW8-5/mCD1d complex stability (Supplemental Fig. 4B). The second factor is that i.m. injection with 7DW8-5 results in more CD1d expression by DCs in dLNs of mice (Fig. 5B). Therefore, two factors, namely the faster and more stable binding to CD1d and the increased expression of CD1d, may independently or in conjunction facilitate 7DW8-5 binding preferentially to CD1d expressed by DCs in the dLNs.

The next question to investigate is how the preferential binding of 7DW8-5 to CD1d-expressing DCs and the increased CD1d expression on DCs (Fig. 5B) would lead to DC activation/maturation in relation to *i*NKT cells (Fig. 5C, 5D). We previously showed that the 7DW8-5/mCD1d complex has a higher binding activity than the αGalCer/mCD1d complex to the TCR of *i*NKT cells, resulting in more potent *i*NKT cell activation (13). In the current study, 7DW8-5 is found to induce *i*NKT cell activation more locally than αGalCer (Fig. 4C, 4D), leading to DC activation/maturation in dLN (Fig. 5C, 5D). In addition to the local activation/maturation of DCs, we found that i.m. injection of 7DW8-5 triggered the recruitment of more DCs to the dLNs than αGalCer (Fig. 5A). I.m. injection of 7DW8-5 results in not only quantitatively more DCs in the dLNs, but those DCs are also qualitatively improved compared with those in αGalCer-treated mice. This was corroborated by the findings that, 7DW8-5 not only recruited more antigen-presenting DCs to the dLNs (Fig. 6C), but also improved activation/maturation of antigen-presenting DCs (Fig. 6D, 6E). These two actions by 7DW8-5 toward DCs in dLNs likely synergistically translate into its potent adjuvant activity. In fact, when we isolated PLN-resident DCs from glycolipid-treated mice and loaded them with a peptide, corresponding to the PyCS-specific CD8+ T-cell epitope, followed by adoptively transferring them to naïve BALB/c mice, a higher level of PyCS-specific CD8+ T-cell response was observed in mice that received the transfer of peptide-loaded PLN-resident DCs from 7DW8-5-treated mice than in mice received those from αGalCer-treated mice (Fig. 5F).

In recent clinical trials, vaccination of human volunteers with a RAS-based malaria vaccine by i.v., but not by intradermal (i.d.) or subcutaneous (s.c.) routes could confer protection (22, 23). I.v. immunization of the RAS vaccine, but not other vaccination routes, is most effective in inducing a high frequency of malaria-specific CD8+ T cells in the liver of non-human primates and mice, and, furthermore, conferring protection in mice (22). It is noteworthy that after an infectious mosquito bite, DCs, particularly those residing in skin-draining LNs, are responsible for priming malaria-specific CD8+ T cells (28). In addition, a number of studies have shown that upon i.d. or s.c immunization, RAS migrates to the draining LN (29–31). Collectively, these studies indicate that not only i.d. and s.c. routes, but also i.m. route of RAS vaccine injection may deliver the parasites to mammals in a manner similar to the bite of malaria-infected mosquitoes. Our studies clearly show that

conjoint administration of 7DW8-5 displays a potent adjuvant effect, enhancing not only the level of malaria-specific CD8+ T-cell response (Fig. 1), but also the level of protective anti-malaria immunity induced by i.m. immunization of IrPySpz to the level similar to that induced by IrPySpz administered i.v. (Tables I and II). Although the level of protection waned 6 weeks after immunization (Table I), the enhancement of the T-cell immunogenicity was observed even 6 weeks after a single immunizing dose of IrPySpz (Fig. 1A, 1B). In future studies, we will test various prime-boost immunization regimens, aiming to determine the optimal IrPySpz prime-boost immunization regimen for the induction of a long lasting protective anti-malaria immunity. Nevertheless, our studies were able to determine the mechanisms underlying the superior adjuvant effect exerted by 7DW8-5, by showing that 7DW8-5 conjointly administered with IrPySpz(GFP-Luc) causes the recruitment of DCs to PLN and induces activation/maturation of PLN-resident PySpz(GFP-Luc)+ DCs, thereby augmenting the induction of PySpz-specific CD8+ T-cell response (Fig. 6G), which leads to an enhanced protective anti-malaria immunity (Fig. 6H).

Importantly, the localized biodistribution of 7DW8-5, which may positively impact its safety profile, has profound significance for clinical applications. In the past decade, αGalCer was tested in clinical trials as a therapy for cancer, hepatitis B and hepatitis C (41–43), and it was reported that some patients experience side effects, such as fever after αGalCer administration likely due to the systemic inflammatory responses induced by αGalCer. In contrast, we show that i.m. injection of 7DW8-5 induces localized activation of *i*NKT cells and DCs without systemic cytokine responses, suggesting that 7DW8-5 may have fewer side effects. In fact, i.m. injection of 7DW8-5 to rhesus macaques only resulted in slight local reactogenicity without systemic side effects (14). Furthermore, it is likely that i.m. injection of 7DW8-5 causes much less anergy and depletion of systemic *i*NKT cells than αGalCer, as demonstrated by the lack of splenic *i*NKT cell activation by 7DW8-5, but not by αGalCer (Fig. 4C), thus adding to 7DW8-5′s attractiveness for future clinical usage.

In conclusion, we found that in contrast with αGalCer, our novel CD1d-binding NKT cell-stimulating glycolipid, 7DW8-5, displays a localized biodistribution upon i.m. administration, by binding more tightly and more rapidly to CD1d molecules expressed by DCs that reside in the dLNs. This localized biodistribution of 7DW8-5 facilitates the activation of *i*NKT cells in the LNs, which in turn, induces activation/maturation of DCs and their recruitment to the dLNs. When 7DW8-5 is co-administered i.m. with a RAS-based rodent malaria vaccine, IrPySpz, 7DW8-5 and the vaccine were found to be not only co-localized in PLNs, but also co-present in the PLN-resident DCs. The quantitative and qualitative improvement of PLN-resident DCs presenting malaria antigens, results in enhancing the levels of malaria-specific CD8+ T-cell response and, ultimately, the level of protective anti-malaria immunity induced by the RAS vaccine. Thus, we systematically demonstrated that the cascade of events initiated by i.m. injection of 7DW8-5 leads to a more potent adjuvant effect. The current findings should be imperative for the future clinical applications of a CD1d-binding *i*NKT-cell ligand, 7DW8-5, as a potent adjuvant for various vaccines.

Supplementary Material

Refer to Web version on PubMed Central for supplementary material.

Acknowledgments

We thank Dr. Vincent Sahi for assisting with FACS analysis and Mr. Ryota Funakoshi for his technical assistance.

This work was supported by grants from the NIH AI070258 (to M.T.) and the Bill and Melinda Gates Foundation Collaboration for AIDS Vaccine Discovery (grant 38648; to D.D.H).

Abbreviations used in this article

αGalCer	α-Galactosylceramide
AF680	Alexa Fluor 680
BTR	BODIPY-Texas Red
DCs	dendritic cells
dLNs	draining lymph nodes
GFP-Luc	GFP-luciferase fusion protein
iNKT	invariant natural killer T
IrPySpz	irradiated Plasmodium yoelii sporozoites
PyCS	Plasmodium yoelii circumsporozoite antigen
PySpz	Plasmodium yoelii sporozoites
PLNs	popliteal lymph nodes
p.i	post injection
RAS	radiation-attenuated whole sporozoites
SAR	structure-activity relationship

References

1. Bendelac A, Savage PB, Teyton L. The biology of NKT cells. Annual review of immunology. 2007; 25:297–336.
2. Kronenberg M. Toward an understanding of NKT cell biology: progress and paradoxes. Annual review of immunology. 2005; 23:877–900.
3. Cerundolo V, Silk JD, Masri SH, Salio M. Harnessing invariant NKT cells in vaccination strategies. Nature reviews Immunology. 2009; 9:28–38.
4. Brigl M, Brenner MB. CD1: antigen presentation and T cell function. Annual review of immunology. 2004; 22:817–890.
5. Venkataswamy MM, Baena A, Goldberg MF, Bricard G, Im JS, Chan J, Reddington F, Besra GS, Jacobs WR Jr, Porcelli SA. Incorporation of NKT cell-activating glycolipids enhances immunogenicity and vaccine efficacy of Mycobacterium bovis bacillus Calmette-Guerin. J Immunol. 2009; 183:1644–1656. [PubMed: 19620317]
6. Huang Y, Chen A, Li X, Chen Z, Zhang W, Song Y, Gurner D, Gardiner D, Basu S, Ho DD, Tsuji M. Enhancement of HIV DNA vaccine immunogenicity by the NKT cell ligand, alpha-galactosylceramide. Vaccine. 2008; 26:1807–1816. [PubMed: 18329757]

7. Ko SY, Ko HJ, Chang WS, Park SH, Kweon MN, Kang CY. alpha-Galactosylceramide can act as a nasal vaccine adjuvant inducing protective immune responses against viral infection and tumor. J Immunol. 2005; 175:3309–3317. [PubMed: 16116223]
8. Hermans IF, Silk JD, Gileadi U, Salio M, Mathew B, Ritter G, Schmidt R, Harris AL, Old L, Cerundolo V. NKT cells enhance CD4+ and CD8+ T cell responses to soluble antigen in vivo through direct interaction with dendritic cells. J Immunol. 2003; 171:5140–5147. [PubMed: 14607913]
9. Fujii S, Shimizu K, Smith C, Bonifaz L, Steinman RM. Activation of natural killer T cells by alpha-galactosylceramide rapidly induces the full maturation of dendritic cells in vivo and thereby acts as an adjuvant for combined CD4 and CD8 T cell immunity to a coadministered protein. The Journal of experimental medicine. 2003; 198:267–279. [PubMed: 12874260]
10. Gonzalez-Aseguinolaza G, Van Kaer L, Bergmann CC, Wilson JM, Schmieg J, Kronenberg M, Nakayama T, Taniguchi M, Koezuka Y, Tsuji M. Natural killer T cell ligand alpha-galactosylceramide enhances protective immunity induced by malaria vaccines. The Journal of experimental medicine. 2002; 195:617–624. [PubMed: 11877484]
11. Anderson BL, Teyton L, Bendelac A, Savage PB. Stimulation of natural killer T cells by glycolipids. Molecules. 2013; 18:15662–15688. [PubMed: 24352021]
12. Fujio M, Wu D, Garcia-Navarro R, Ho DD, Tsuji M, Wong CH. Structure-based discovery of glycolipids for CD1d-mediated NKT cell activation: tuning the adjuvant versus immunosuppression activity. Journal of the American Chemical Society. 2006; 128:9022–9023. [PubMed: 16834361]
13. Li X, Fujio M, Imamura M, Wu D, Vasan S, Wong CH, Ho DD, Tsuji M. Design of a potent CD1d-binding NKT cell ligand as a vaccine adjuvant. Proceedings of the National Academy of Sciences of the United States of America. 2010; 107:13010–13015. [PubMed: 20616071]
14. Padte NN, Boente-Carrera M, Andrews CD, McManus J, Grasperge BF, Gettie A, Coelho-dos-Reis JG, Li X, Wu D, Bruder JT, Sedegah M, Patterson N, Richie TL, Wong CH, Ho DD, Vasan S, Tsuji M. A glycolipid adjuvant, 7DW8-5, enhances CD8+ T cell responses induced by an adenovirus-vectored malaria vaccine in non-human primates. PloS one. 2013; 8:e78407. [PubMed: 24205224]
15. Xu X, Hegazy W, Guo L, Gao X, Courtney AN, Kurbanov S, Liu D, Tian G, Manuel ER, Diamond DJ, Hensel M, Metelitsa LS. Development of an Effective Cancer Vaccine Using Attenuated Salmonella and Type III Secretion System to Deliver Recombinant Tumor-Associated Antigens. Cancer research. 2014; 74:6260–6270. [PubMed: 25213323]
16. Venkataswamy MM, Ng TW, Kharkwal SS, Carreno LJ, Johnson AJ, Kunnath-Velayudhan S, Liu Z, Bittman R, Jervis PJ, Cox LR, Besra GS, Wen X, Yuan W, Tsuji M, Li X, Ho DD, Chan J, Lee S, Frothingham R, Haynes BF, Panas MW, Gillard GO, Sixsmith JD, Korioth-Schmitz B, Schmitz JE, Larsen MH, Jacobs WR Jr, Porcelli SA. Improving Mycobacterium bovis Bacillus Calmette-Guerin as a Vaccine Delivery Vector for Viral Antigens by Incorporation of Glycolipid Activators of NKT Cells. PloS one. 2014; 9:e108383. [PubMed: 25255287]
17. Padte NN, Li X, Tsuji M, Vasan S. Clinical development of a novel CD1d-binding NKT cell ligand as a vaccine adjuvant. Clin Immunol. 2011; 140:142–151. [PubMed: 21185784]
18. Hoffman SL, Goh LM, Luke TC, Schneider I, Le TP, Doolan DL, Sacci J, de la Vega P, Dowler M, Paul C, Gordon DM, Stoute JA, Church LW, Sedegah M, Heppner DG, Ballou WR, Richie TL. Protection of humans against malaria by immunization with radiation-attenuated Plasmodium falciparum sporozoites. The Journal of infectious diseases. 2002; 185:1155–1164. [PubMed: 11930326]
19. Herrington D, Davis J, Nardin E, Beier M, Cortese J, Eddy H, Losonsky G, Hollingdale M, Sztein M, Levine M, et al. Successful immunization of humans with irradiated malaria sporozoites: humoral and cellular responses of the protected individuals. The American journal of tropical medicine and hygiene. 1991; 45:539–547. [PubMed: 1951863]
20. Gwadz RW, Cochrane AH, Nussenzweig V, Nussenzweig RS. Preliminary studies on vaccination of rhesus monkeys with irradiated sporozoites of Plasmodium knowlesi and characterization of surface antigens of these parasites. Bulletin of the World Health Organization. 1979; 57(Suppl 1): 165–173. [PubMed: 120766]

21. Nussenzweig RS, Vanderberg J, Most H, Orton C. Protective immunity produced by the injection of x-irradiated sporozoites of plasmodium berghei. Nature. 1967; 216:160–162. [PubMed: 6057225]

22. Epstein JE, Tewari K, Lyke KE, Sim BK, Billingsley PF, Laurens MB, Gunasekera A, Chakravarty S, James ER, Sedegah M, Richman A, Velmurugan S, Reyes S, Li M, Tucker K, Ahumada A, Ruben AJ, Li T, Stafford R, Eappen AG, Tamminga C, Bennett JW, Ockenhouse CF, Murphy JR, Komisar J, Thomas N, Loyevsky M, Birkett A, Plowe CV, Loucq C, Edelman R, Richie TL, Seder RA, Hoffman SL. Live attenuated malaria vaccine designed to protect through hepatic CD8(+) T cell immunity. Science. 2011; 334:475–480. [PubMed: 21903775]

23. Seder RA, Chang LJ, Enama ME, Zephir KL, Sarwar UN, Gordon IJ, Holman LA, James ER, Billingsley PF, Gunasekera A, Richman A, Chakravarty S, Manoj A, Velmurugan S, Li M, Ruben AJ, Li T, Eappen AG, Stafford RE, Plummer SH, Hendel CS, Novik L, Costner PJ, Mendoza FH, Saunders JG, Nason MC, Richardson JH, Murphy J, Davidson SA, Richie TL, Sedegah M, Sutamihardja A, Fahle GA, Lyke KE, Laurens MB, Roederer M, Tewari K, Epstein JE, Sim BK, Ledgerwood JE, Graham BS, Hoffman SL. Protection against malaria by intravenous immunization with a nonreplicating sporozoite vaccine. Science. 2013; 341:1359–1365. [PubMed: 23929949]

24. Miller JL, Murray S, Vaughan AM, Harupa A, Sack B, Baldwin M, Crispe IN, Kappe SH. Quantitative bioluminescent imaging of pre-erythrocytic malaria parasite infection using luciferase-expressing Plasmodium yoelii. PloS one. 2013; 8:e60820. [PubMed: 23593316]

25. Smiley ST, Kaplan MH, Grusby MJ. Immunoglobulin E production in the absence of interleukin-4-secreting CD1-dependent cells. Science. 1997; 275:977–979. [PubMed: 9020080]

26. Jung S, Unutmaz D, Wong P, Sano G, De los Santos K, Sparwasser T, Wu S, Vuthoori S, Ko K, Zavala F, Pamer EG, Littman DR, Lang RA. In vivo depletion of CD11c+ dendritic cells abrogates priming of CD8+ T cells by exogenous cell-associated antigens. Immunity. 2002; 17:211–220. [PubMed: 12196292]

27. Schmieg J, Yang G, Franck RW, Van Rooijen N, Tsuji M. Glycolipid presentation to natural killer T cells differs in an organ-dependent fashion. Proceedings of the National Academy of Sciences of the United States of America. 2005; 102:1127–1132. [PubMed: 15644449]

28. Amino R, Thiberge S, Martin B, Celli S, Shorte S, Frischknecht F, Menard R. Quantitative imaging of Plasmodium transmission from mosquito to mammal. Nature medicine. 2006; 12:220–224.

29. Chakravarty S, Cockburn IA, Kuk S, Overstreet MG, Sacci JB, Zavala F. CD8+ T lymphocytes protective against malaria liver stages are primed in skin-draining lymph nodes. Nature medicine. 2007; 13:1035–1041.

30. Yamauchi LM, Coppi A, Snounou G, Sinnis P. Plasmodium sporozoites trickle out of the injection site. Cellular microbiology. 2007; 9:1215–1222. [PubMed: 17223931]

31. Obeid M, Franetich JF, Lorthiois A, Gego A, Gruner AC, Tefit M, Boucheix C, Snounou G, Mazier D. Skin-draining lymph node priming is sufficient to induce sterile immunity against pre-erythrocytic malaria. EMBO molecular medicine. 2013; 5:250–263. [PubMed: 23255300]

32. Sullivan BA, Nagarajan NA, Wingender G, Wang J, Scott I, Tsuji M, Franck RW, Porcelli SA, Zajonc DM, Kronenberg M. Mechanisms for glycolipid antigen-driven cytokine polarization by Valpha14i NKT cells. J Immunol. 2010; 184:141–153. [PubMed: 19949076]

33. Schmidt NW, Butler NS, Badovinac VP, Harty JT. Extreme CD8 T cell requirements for anti-malarial liver-stage immunity following immunization with radiation attenuated sporozoites. PLoS Pathog. 2010; 6:e1000998. [PubMed: 20657824]

34. Liang PH, Imamura M, Li X, Wu D, Fujio M, Guy RT, Wu BC, Tsuji M, Wong CH. Quantitative microarray analysis of intact glycolipid-CD1d interaction and correlation with cell-based cytokine production. Journal of the American Chemical Society. 2008; 130:12348–12354. [PubMed: 18712867]

35. Vo-Hoang Y, Micouin L, Ronet C, Gachelin G, Bonin M. Total enantioselective synthesis and in vivo biological evaluation of a novel fluorescent BODIPY alpha-galactosylceramide. Chembiochem : a European journal of chemical biology. 2003; 4:27–33. [PubMed: 12512073]

36. Yu KO, Im JS, Illarionov PA, Ndonye RM, Howell AR, Besra GS, Porcelli SA. Production and characterization of monoclonal antibodies against complexes of the NKT cell ligand alpha-

galactosylceramide bound to mouse CD1d. Journal of immunological methods. 2007; 323:11–23. [PubMed: 17442335]

37. Annoura T, Chevalley S, Janse CJ, Franke-Fayard B, Khan SM. Quantitative analysis of Plasmodium berghei liver stages by bioluminescence imaging. Methods in molecular biology. 2013; 923:429–443. [PubMed: 22990796]
38. Ploemen IH, Prudencio M, Douradinha BG, Ramesar J, Fonager J, van Gemert GJ, Luty AJ, Hermsen CC, Sauerwein RW, Baptista FG, Mota MM, Waters AP, Que I, Lowik CW, Khan SM, Janse CJ, Franke-Fayard BM. Visualisation and quantitative analysis of the rodent malaria liver stage by real time imaging. PloS one. 2009; 4:e7881. [PubMed: 19924309]
39. Zajonc DM, Cantu C 3rd, Mattner J, Zhou D, Savage PB, Bendelac A, Wilson IA, Teyton L. Structure and function of a potent agonist for the semi-invariant natural killer T cell receptor. Nature immunology. 2005; 6:810–818. [PubMed: 16007091]
40. Koch M V, Stronge S, Shepherd D, Gadola SD, Mathew B, Ritter G, Fersht AR, Besra GS, Schmidt RR, Jones EY, Cerundolo V. The crystal structure of human CD1d with and without alpha-galactosylceramide. Nature immunology. 2005; 6:819–826. [PubMed: 16007090]
41. Woltman AM, Ter Borg MJ, Binda RS, Sprengers D, von Blomberg BM, Scheper RJ, Hayashi K, Nishi N, Boonstra A, van der Molen R, Janssen HL. Alpha-galactosylceramide in chronic hepatitis B infection: results from a randomized placebo-controlled Phase I/II trial. Antiviral therapy. 2009; 14:809–818. [PubMed: 19812443]
42. Kunii N, Horiguchi S, Motohashi S, Yamamoto H, Ueno N, Yamamoto S, Sakurai D, Taniguchi M, Nakayama T, Okamoto Y. Combination therapy of in vitro-expanded natural killer T cells and alpha-galactosylceramide-pulsed antigen-presenting cells in patients with recurrent head and neck carcinoma. Cancer science. 2009; 100:1092–1098. [PubMed: 19302288]
43. Veldt BJ, van der Vliet HJ, von Blomberg BM, van Vlierberghe H, Gerken G, Nishi N, Hayashi K, Scheper RJ, de Knegt RJ, van den Eertwegh AJ, Janssen HL, van Nieuwkerk CM. Randomized placebo controlled phase I/II trial of alpha-galactosylceramide for the treatment of chronic hepatitis C. Journal of hepatology. 2007; 47:356–365. [PubMed: 17599630]

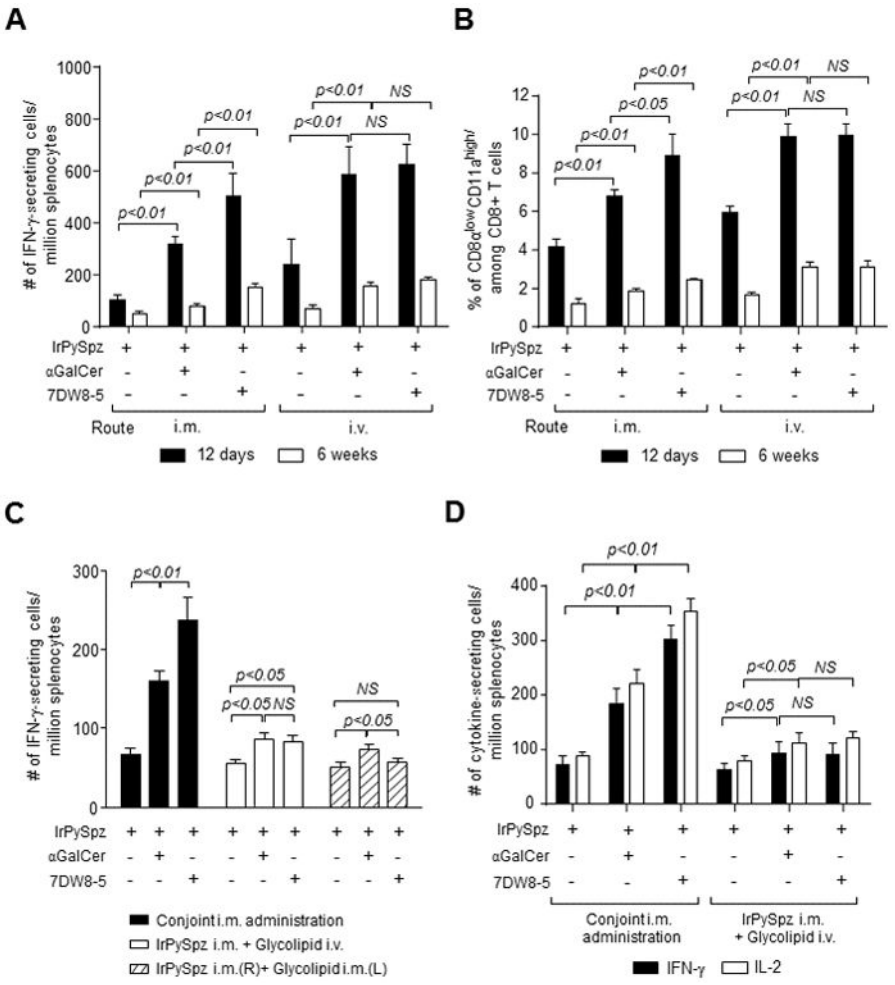

FIGURE 1.

The potent 7DW8-5 adjuvant effect is dependent on the route of its administration. In (A and B), groups of 4 BALB/c mice were administered i.m. (anterior tibialis muscles) or i.v. (tail vein) with 1×10^4 IrPySpz alone or conjointly with 1 μg αGalCer or 7DW8-5. Twelve days (solid column) or 6 weeks (unfilled column) later, splenocytes were harvested, and the relative number of PyCS-specific CD8+ T cells was determined with an IFN-γ ELISpot assay in (A) or the percentage of $CD8\alpha^{low}CD11a^{high}$ CD8+ T cells per total CD8+ T cells was determined by flow cytometric analysis in (B). In (C), groups of 4 BALB/c mice were administered i.m. with 1×10^4 IrPySpz alone or conjointly with 1 μg αGalCer or 7DW8-5 by i.m. or i.v. The solid column represents conjoint i.m. administration of the vaccine and each respective glycolipid; the unfilled column represents i.m. administration of the vaccine, immediately followed i.v. administration of each glycolipid; the striped column represents i.m. administration of the vaccine and glycolipid in opposite legs. Twelve days later, splenocytes were harvested, and the relative number of PyCS-specific CD8+ T cells was determined with an IFN-γ ELISpot assay. In (D), groups of 4 BALB/c mice were administered i.m. with 1×10^4 IrPySpz alone or conjointly with 1 μg αGalCer or 7DW8-5 by i.m. or i.v., and 12 days later, splenocytes were harvested, and the relative number of PyCS-

specific CD8+ T cells was determined with IFN-γ and IL-2 ELISpot assays. In (A–D), the results are expressed as mean ± S.D of four mice in each group.

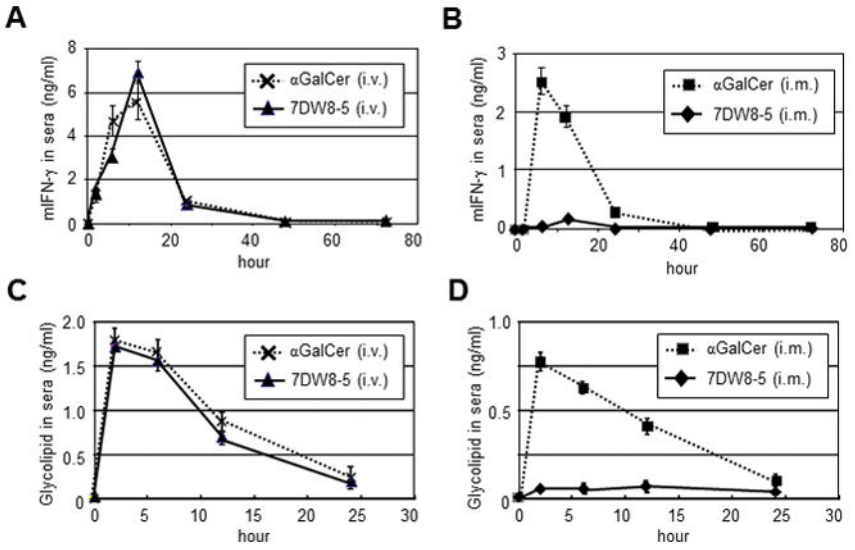

FIGURE 2.

The levels of mouse IFN-γ and glycolipids in the sera of glycolipid-administered mice. In (A and B), after BALB/c mice (n=5/group) were administered 1 μg αGalCer or 7DW8-5 by i.v. (A) or i.m. (B) injection, sera were obtained at indicated time points, and the concentrations of murine IFN-γ in the sera were determined by an ELISA. In (C and D), glycolipid serum concentrations were assessed by co-culturing 3×10^4 murine 1.2 *i*NKT hybridoma cells and 3×10^4 A20-mCD1d for 16 hr in a 96-well plate in the presence of serial dilutions of individual sera collected from mice injected with 1 μg αGalCer or 7DW8-5 by i.v. (E) or i.m. (F). Supernatants were analyzed for IL-2 concentrations by ELISA. Glycolipid concentrations were calculated from standard curves generated from the serially diluted glycolipids. Mean ± SD of five mice at each time point is shown.

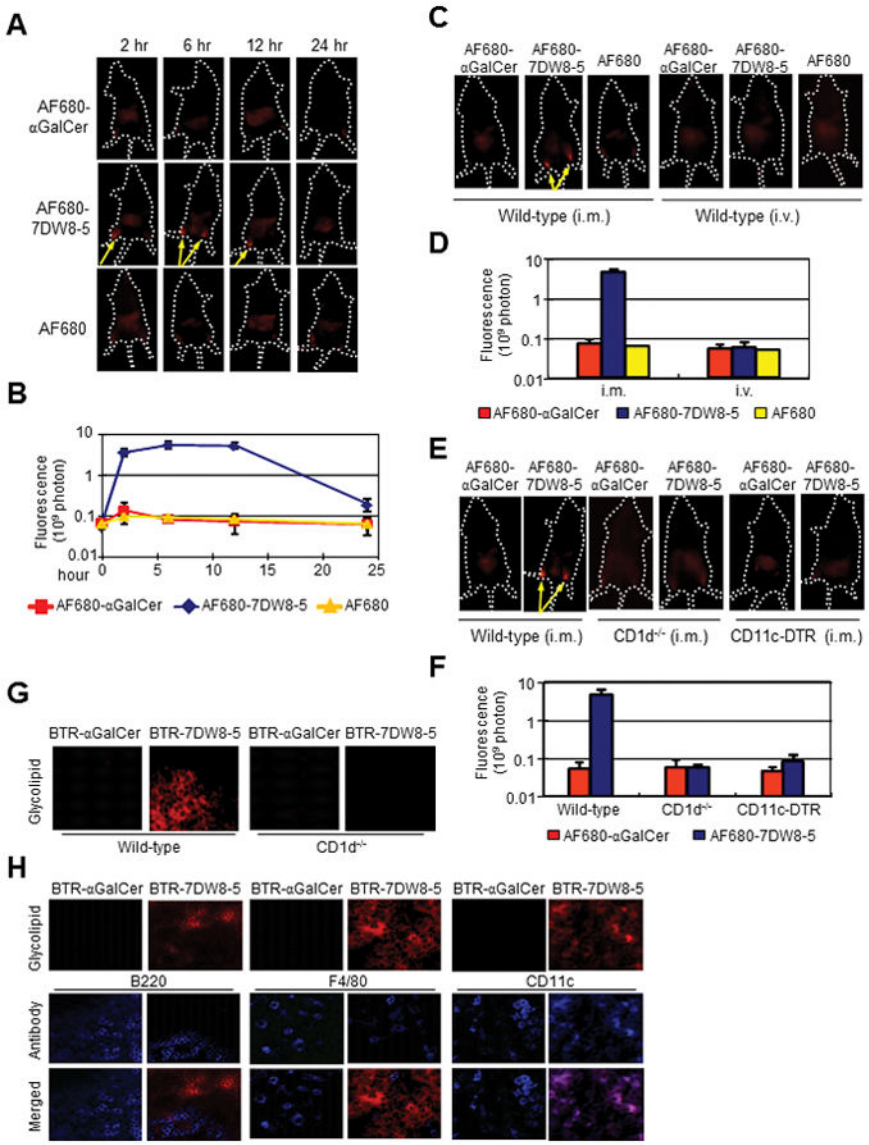

FIGURE 3.

7DW8-5 is retained locally following i.m. injection and PLN-resident DCs present 7DW8-5 in a CD1d-dependent manner. (A and B) BALB/c mice (n=5/group) were injected i.m. (anterior tibialis muscles) with 5 μg AF680-αGalCer, AF680-7DW8-5 or AF680, and imaged over a time course with Lumina IVIS. (C and D) Effects of administration route on biodistribution were determined by imaging mice 8 hr after i.m. or i.v. injection of AF680-αGalCer, AF680-7DW8-5 or AF680. (E and F) CD1d$^{-/-}$ and CD11c-DTR mice were given AF680-labeled glycolipids by i.m. injection and imaged 8 hr later. (A, C, E) Representative images from one mouse per group are shown; yellow arrows indicate high fluorescence intensities. (B, D, F) Fluorescence intensities of the anterior tibialis muscles were quantified, and mean ± SD of five mice is shown. (G) BALB/c and CD1d$^{-/-}$ mice (n=5/group) were administered 2 μg BTR-αGalCer or BTR-7DW8-5 by i.m. injection. Eight-hours later, PLNs were isolated and sections were prepared for image analysis. (H) BALB/c mice (n=5/group) were treated as in (G), PLNs were isolated and stained with anti-B220, anti-F4/80 and anti-

CD11c antibodies to visualize B cells, macrophages and DCs, respectively. In both (G and H), images were collected using a LSM510 confocal microscope. Images from one representative mouse are shown.

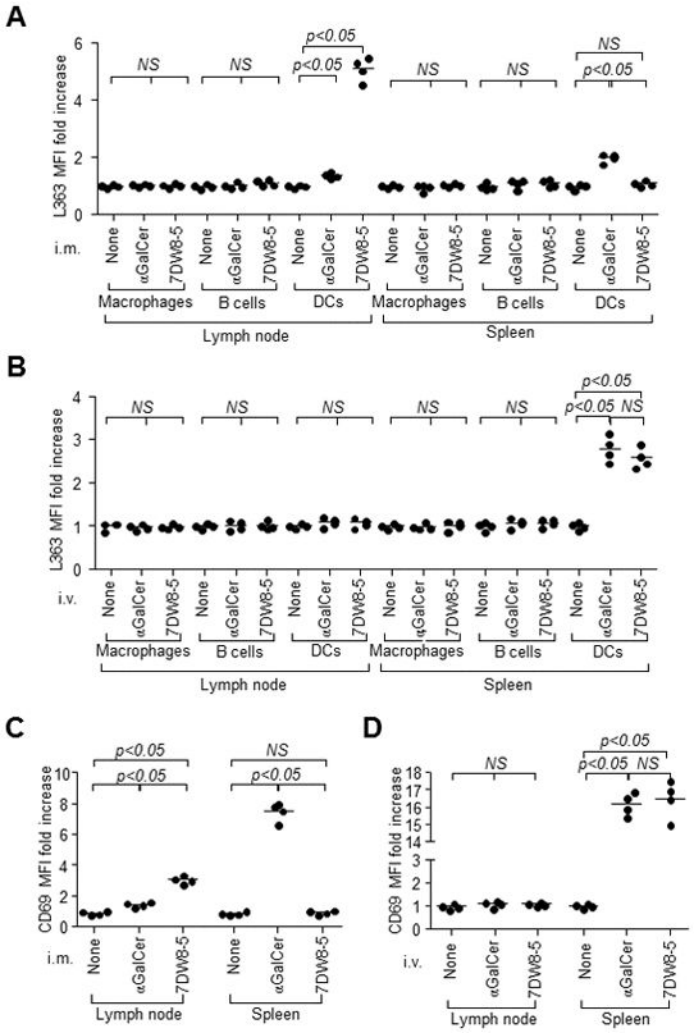

FIGURE 4.

7DW8-5 is primarily presented by PLN-resident DCs and induces *i*NKT cell activation in PLNs following i.m. injection. BALB/c mice (n=4/group) were administered 1 μg αGalCer or 7DW8-5 by (A) i.m. or (B) i.v. injection. PLNs and spleens were isolated 6 hr later, and CD1d-bound glycolipid on macrophages, B cells and DCs were stained with L363 and quantified by a flow cytometry. The results are expressed as fold increase of L363 MFI compared with untreated mice. BALB/c mice (n=4/group) were injected (C) i.m. or (D) i.v. with 1 μg αGalCer or 7DW8-5. Two hr later, PLNs and spleens were isolated, and *i*NKT cell activation was assessed by monitoring CD69 expression using flow cytometry. The CD69 MFI fold increase over mice is shown.

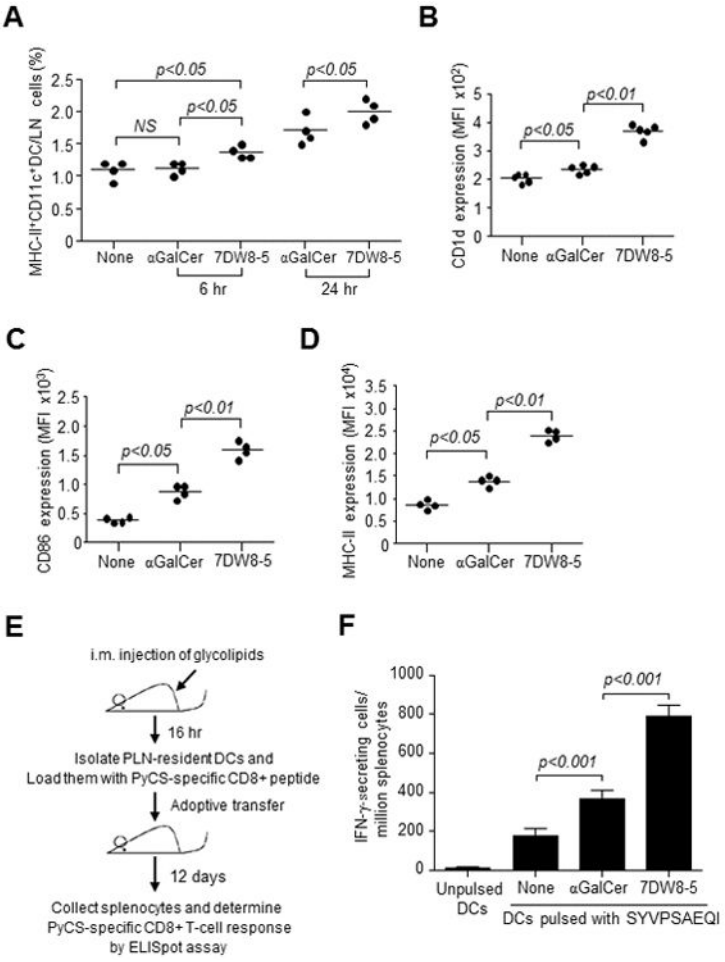

FIGURE 5.

Localized biodistribution of 7DW8-5 recruits more DCs and increases DC activation/maturation leading to an increased malaria-specific CD8+ T-cell response compared with αGalCer. BALB/c mice (n=4/group) were injected i.m. with vehicle DMSO, 1 μg αGalCer or 7DW8-5. (A) PLNs were isolated at 6 and 24 hr after injection, and the percentage of MHC-II$^+$ CD11c$^+$ DCs was quantified with flow cytometry. (B) CD1d (C) CD86 and (D) MHC-II expression by DCs isolated from PLNs 16 hr p.i, were also analyzed by a flow cytometry. Data for individual mice are shown; line represents mean. (E and F) The antigen presenting capability of DCs from PLNs was determined by an adoptive transfer. (E) BALB/c mice (n=20/group) were injected i.m. with 1 μg glycolipid, and 16 hr later, CD11c$^+$ DCs were isolated from the pooled PLNs and loaded with 30 μg/ml SYVPSAEQI peptide for 1 hr at 37°C. Seven hundred fifty thousand DCs were adoptively transferred i.v. to each of naïve BALB/c mice (n=4/group). (F) Twelve days later, the PyCS-specific CD8+ T-cell response induced in transferred mice was determined by an IFN-γ ELISpot assay. Mean ± S.D of four mice in each group is shown.

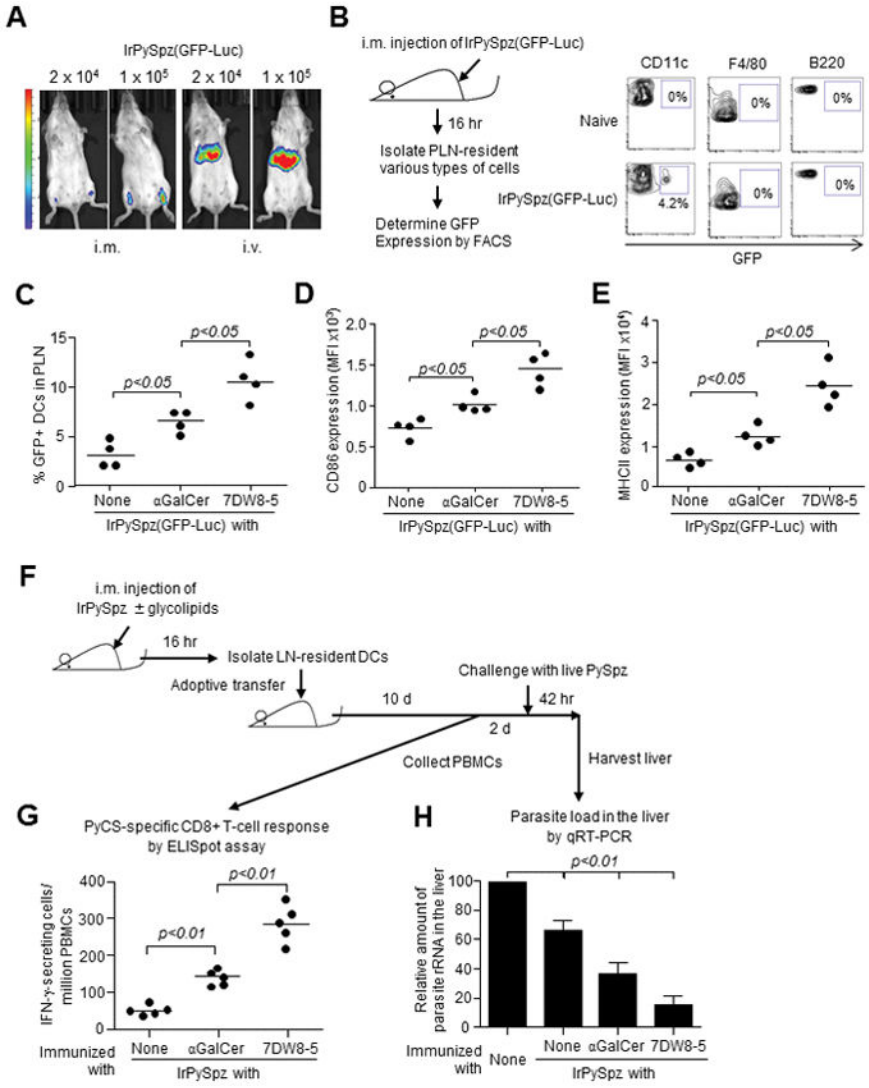

FIGURE 6.

Co-localization of 7DW8-5 and IrPySpz in dLN-resident DCs facilitates activation and recruitment of DCs and enhances T-cell immunogenicity and efficacy of IrPySpz vaccine. (A) BALB/c mice (n=4/group) were injected i.m. or i.v. with 2×10^4 or 1×10^5 IrPySpz(GFP-Luc). Twelve hr later, mice were injected i.p. with 3 mg D-luciferin, and the luciferin signal was detected using Lumina IVIS. Images from one representative mouse are shown. (B) BALB/c mice (n=4/group) were injected i.m. with 1×10^5 IrPySpz(GFP-Luc). Sixteen hr later, lymphocytes were isolated from PLNs, and GFP expression in DCs, macrophages and B cells from total lymphocytes were determined by a flow cytometry. Naïve mice were used as a negative control. Data from one representative mouse in each group is shown. (C–E) BALB/c mice (n=4/group) were injected i.m. with 1×10^5 IrPySpz(GFP-Luc).alone or together with 1 μg of each glycolipid. Sixteen hr later, lymphocytes were isolated from PLNs and (C) the percentage of GFP^+ DCs among total lymphocytes, as well as (D) CD86 and (E) MHC-II expression on GFP^+ PLNs-resident DCs were determined. Data for individual mice are shown; line represents mean. (F) BALB/c mice (n=25/group) were

immunized i.m. with 1×10^5 IrPySpz(GFP-Luc) alone or together with 1 μg of each glycolipid. Sixteen hr later, PLNs-resident DCs were isolated and then 7.5×10^5 DCs/mouse were adoptively transferred i.v. to naïve BALB/c mice (n=5/group). (G) Ten days later, blood was collected and the PyCS-specific CD8+ T-cell response determined by an IFN-γ ELISpot assay. (H) Two days later the same transferred mice and naïve BALB/c mice as controls were i.v challenged with 2×10^4 PySpz and 42 hr later, the parasite burden in liver was determined by quantifying the amount of parasite-specific rRNA by a real-time qRT-PCR. Mean ± S.D of five mice in each group is shown.

Table I

Co-administration of 7DW8-5 by i.m. but not i.v. significantly enhances protective immunity induced IrPySpz

Vaccine + Adjuvant	Administration Route	Immunization-challenge Interval	Protected/Challenged	*P* value‡
Naïve			0/10	
IrSpz	i.m.	12 days	0/5	
IrPySpz + αGalCer	i.m. conjointly administered		1/5	0.29 *(NS)*
IrPySpz + 7DW8-5			3/5	0.038*
IrSpz	i.v.		2/5	
IrPySpz + αGalCer	i.v. conjointly administered		4/5	0.20 *(NS)*
IrPySpz + 7DW8-5			3/5	0.53 *(NS)*
IrSpz	i.m.	6 weeks	0/5	
IrPySpz + αGalCer	i.m. conjointly administered		0/5	- *(NS)*
IrPySpz + 7DW8-5			0/5	- *(NS)*
IrSpz	i.v.		0/5	
IrPySpz + αGalCer	i.v. conjointly administered		1/5	0.29 *(NS)*
IrPySpz + 7DW8-5			1/5	0.29 *(NS)*

‡*P* value between IrPySpz alone group and IrPySpz + glycolipid group was calculated by χ^2 test, using 2 × 2 contingency table (degree of freedom = 1).

*P<0.05;

NS means “not significant.”

Table II

Conjoint i.m. administration of 7DW8-5 potently enhances protective immunity induced IrPySpz

Vaccine + Adjuvant	Administration Route	Immunization-challenge Interval	Protected/Challenged	*P* value‡
Naïve			0/10	
IrSpz	i.m.	12 days	2/10	
IrPySpz + αGalCer	i.m. conjointly administered		7/10	0.025*
IrPySpz + 7DW8-5			9/10	0.0017**
IrPySpz + αGalCer	i.m. (IrPySpz) + i.v. (Glycolipid)		4/10	0.33 *(NS)*
IrPySpz + 7DW8-5			4/10	0.33 *(NS)*
IrPySpz + αGalCer	i.m. (R: IrPySpz) + i.m. (L: Glycolipid)		4/10	0.33 *(NS)*
IrPySpz + 7DW8-5			2/10	- *(NS)*
IrSpz	i.v.		9/10	

‡*P* value between IrPySpz alone group and IrPySpz + glycolipid group was calculated by χ^2 test, using 2 × 2 contingency table (degree of freedom = 1).

*P<0.05;

**P<0.01;

NS means "not significant." R, right leg; L, left leg.